ce/papers Proceedings in civil engineering

Ernst & Sohn A Wiley Brand

ORIGINAL ARTICLE

eurosteel AMSTERDAM 2023

Ernst & Sohn A Wiley Brand

Seismic behaviour of dissipative beam-to-column steel and steel-concrete composite joints

Georgios Skarmoutsos[1] | Ulrike Kuhlmann[1]

Correspondence

Dipl. Eng. Georgios Skarmoutsos
University of Stuttgart
Institute of Structural Design
Pfaffenwaldring 7
70569 Stuttgart
Email: georgios.skarmoutsos@ke.uni-stuttgart.de

[1] University of Stuttgart, Institute of Structural Design, Germany

Abstract

The present paper deals with the seismic behaviour of bolted steel and steel-concrete composite partial-strength beam-to-column joints with endplate connections. In a series of experiments in total 12 two-sided internal joint specimens were tested, of which 3 were all-steel and 9 steel-concrete composite. For those, 5 parameters were varied, **(i)** thickness of endplate $\mathbf{t_{ep}}$, **(ii)** vertical distance of T-stub bolt rows $\mathbf{e_4}$, **(iii)** distance of first shear stud to face of the endplate **l**, **(iv)** reinforcement ratio of concrete slab **ρ** and **(v)** number of bolt rows. The design of the specimens was performed with the help of both the component model as given in EN 1993-1-8 and a FEM model. The chosen parameter values were optimised to provide, for given beam and column sections, an upper and lower limit regarding moment capacity and rotational stiffness, for sufficient energy dissipation and ductility. The experimental results show that the stiffness of the concrete slab leads to a significantly different response of composite compared to all-steel joints, especially regarding rotational stiffness and capacity of the joint as well as flexural stiffness of the (composite) beams. The composite joints present an overall better seismic behaviour compared to all-steel ones.

Keywords

Steel-concrete composite, dissipative joints, partial-strength joints, seismic design

1 Introduction

The idea behind the experimental work presented herein, which is part of [1], was to start from beam-to-column joint configurations commonly used in non-seismic or low-seismicity areas and by applying on them the minimum necessary modifications to transform them into dissipative partial-strength joints that can be implemented in moment resisting frames located in areas of up to medium seismicity. To achieve that, close attention was paid in the pre-design stage to literature related to design for robustness and non-seismic areas, [2], [3], [4], [5], [6], [7], to literature for seismic design and design of dissipative joints [8], [9], literature for the design of joints [10], [11] and to the standards [12], [13], [14], [15], [16], [17]. Modifications considered as necessary for double-sided internal joints are (i) the strengthening of the columns, possibly also use of stronger profile series, (ii) strengthening of welds and bolts, (iii) the application of strength hierarchy criteria to allow for activation of the connections and (iv) if possible the design of symmetrical connections.

The specimens were designed with the help of the component model as given in [12] and [13] and of a refined FEM model for all-steel joints, which provided the joint behaviour in the non-linear area. The exact parameter values used for the dimensioning of the specimens tested were extracted out of the FEM model results.

In the following sections a short description of the experiments, a part of the experimental results and some of the drawn conclusions together with a short critical discussion are given.

2 Description of the tests

2.1 Tested specimens

The experimental series contained in total 3 all-steel and 9 steel-concrete composite double-sided joints, see Table 1 and 2. One of the composite joints, experiment No. 4 see Table 2, was tested under monotonic static loading, whereas the rest were tested under quasi-static cyclic loading according to the loading protocol of [15], modified with 2 additional load steps at 25 mrad and 35 mrad (2 load cycles at each step). The parameters varied were the column and beam profile section, the thickness of the endplate t_{ep}, the vertical distance of bolt rows e_4, the reinforcement ratio ρ of the concrete slab, the distance between the first shear stud and the face of the column l and the number of bolt rows. More information about the influence of parameters on the response of the joints are

available in [18].

Table 1 Conventions – name of specimens

Column	Beam	t_{ep}	e_4	l	ρ	Bolt rows
HEA300-**HA30** **S**teel or **C**omposite	IPE300-**I30** **S**teel or **C**omposite	(in mm)				3 or 4

Table 2 Tested specimens

Specimens (Steel grade S355J2 – Concrete class C30/37)			
1	HB30S-HA24S-15-100	7	HA30Cst-I30C-20-100-450-ρ2
2	HB30S-HA24S-20-100	8	HA30Cst-I30C-15-100-450-ρ1
3	HB30S-HA24S-20-130	9	HA30Cst-I30C-20-100-170-ρ2
4	HA30C-I30C-20-150-450-ρ2	10	HA30Cst-I30C-20-150-170-ρ2
5	HA30S-I30C-20-150-450-ρ2	11	HA30Cst-I30C-15-100-450-ρ2
6	HA30C-I30C-20-150-450-ρ2	12	HA30S-I30C-15-100-450-ρ2-3br

2.2 Test setup & instrumentation

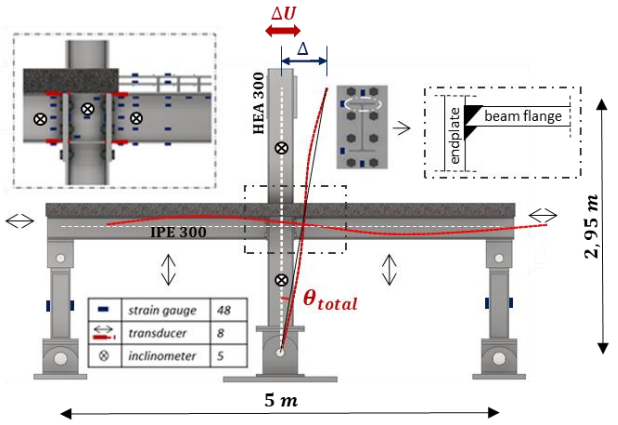

Figure 1 Measurement equipment, boundary conditions and type of beam-to-endplate welds.

In total around 60 channels per experiment were used for approximately 48 strain gauges, 8 transducers and 5 inclinometers, see Figure 1, providing the stress and deformation state for nearly every component of the connection. The contribution of the components panel zone, in terms of γ, and beam θ_b, see Figure 2, to the total joint rotation θ_{total} presented in the following section 3.3 were calculated according to the following equations:

$$\gamma = \theta_{total} - incm_{colpz} \quad (1)$$

$$\theta_b = incm_{beam} \quad (2)$$

Where $incm_{beam}$ and $incm_{colpz}$ stand for the measurements of the inclinometers applied on the beam and column panel zone, respectively. Hence, the rotation angle of the composite beam due to shear deformation of the web panel has been neglected. The derivation of θ_{pz} and θ_c, as given in [19] see Figure 2, is in development.

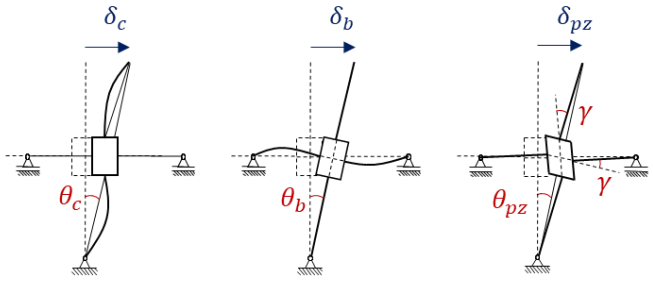

Figure 2 Explanation of θc, θb, θpz and γ according to [19].

Figure 3 Concrete slab steel reinforcement arrangement in the area of connection, use of polysterene for the construction of an opening in the concrete slab around the column, see also Figure 14.

3 Experimental results

3.1 All-steel joints

All 3 tested all-steel joints presented a very ductile behaviour, reaching rotations far further than the minimum plastic rotation capacity of 15 mrad and 25 mrad, see Figure 4, required by [14] for areas of low and medium seismicity. Through the use of larger bolt diameters, M30, the premature failure of the bolts was successfully prevented, while the design of the beam-to-column welds according to [9] successfully prevented an early failure of the welds. Interesting conclusions have also been drawn for the behaviour of the bolts in endplate connections and under large deformations of the endplate. The need for a ductility criterion that considers aside from the strength also the deformation capacity of the connection and of its components (mainly bolts and endplates), for the cases where high connection ductility is required, is expressed in [18].

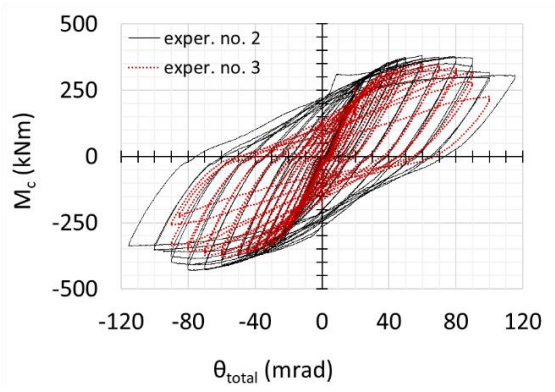

Figure 4 Comparison of M-θ_{total} curves for experiments No. 2 & No. 3. Good dissipative and highly ductile behaviour for both experiments, formation of plastic hinge in the beams for experiment No. 2 is of advantage in terms of energy dissipation and ductility.

Although the tested partial-strength all-steel joints exhibited a very ductile behaviour, it should be noted that the dissipative behaviour started for values higher than $\theta_{total} = 20\,mrad$. Use of larger steel profiles with increased flexural

stiffness could possibly allow for reduced vertical deflection of the beams and earlier activation of the endplates. The vertical deflection in the middle of the beam length of an all-steel joint (here plotted up to 45 mrad), experiment No. 2, compared to those of a composite joint, experiment No.9, are given in Figure 5.

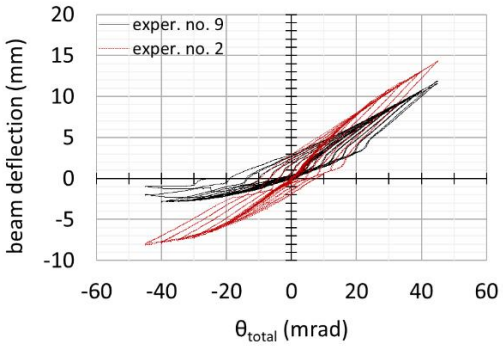

Figure 5 Measured beam deflection in the middle of beam's length for an all steel joint, No. 2, and a composite one, No. 9. Concrete slab significantly restrains the rotation of composite beam and endplates.

Regarding all-steel joints the components of endplate, beams, panel zone and column have been activated, with the endplates and the panel zone having the major contributions. The contribution of the different components will be presented only for some of the composite specimens in Chapter 3.3.

3.2 Composite steel-concrete joints

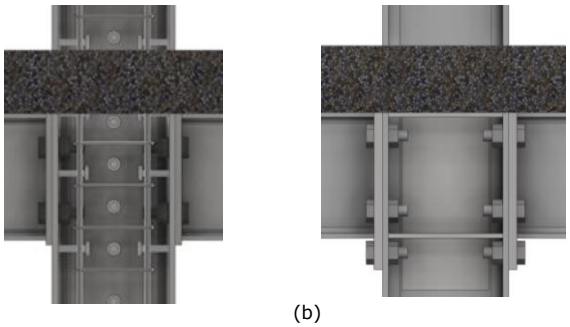

(a) (b)

Figure 6 (a) Composite column configuration, intended to satisfy also normative requirements for fire safety. (b) all-steel column configuration with supplementary web plates and stiffeners.

Regarding the tested steel-concrete composite joints, their seismic behaviour strongly depends on the column configuration used in each of the specimens. More specifically, originally 2 column configurations were planned, one with a steel HEA300 profile including also supplementary web plates and stiffeners, see Figure 6b, and another as composite configuration. The composite configuration was a partially encased concrete filled HEA300 with additionally longitudinal rebars, stirrups running through the column web and shear studs in the area of connection both on the column flanges and web. The latter configuration was intended to satisfy also normative requirements for fire safety. A sketch of the composite column configuration, without the concrete infill, is given in Figure 6a.

After testing the first two specimens with composite column configuration, No. 4 and 6, it was observed that although the steel reinforcement and shear studs on flanges and web of the column effectively prevented any significant cracks in the concrete core up to at least $\theta_{total} = 45\,mrad$, the stiffness of the column web panel zone was inadequate to allow for a proper activation of the connection.

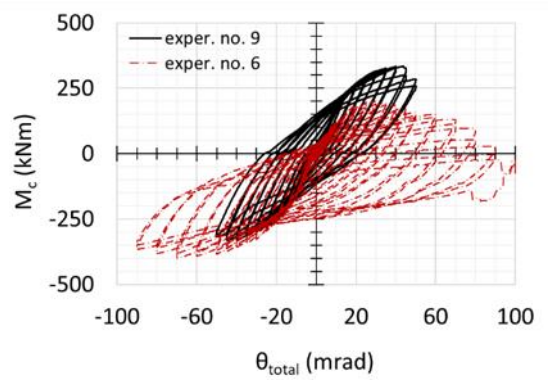

Figure 7 Comparison of M-θ_{total} curves for experiments No. 6 (composite column) & No. 9 (stiffened composite column). $M^{+}_{exp.no.6} \approx 0{,}6 \cdot M^{+}_{exp.no.9}$. Weak column web panel zone of experiment No. 6 does not allow for full activation of the connection, see also Figure 8a.

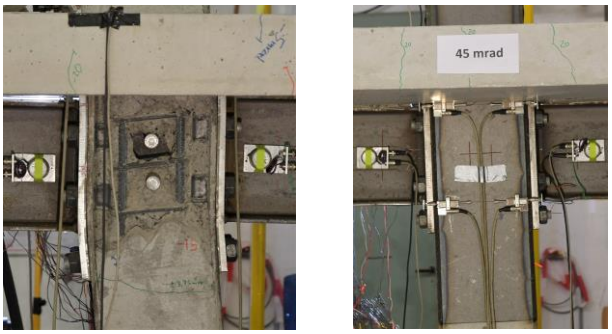

(a) (b)

Figure 8 (a) Deformation of joint No. 6 at $\theta_{total} = 90\,mrad$. Soft behaviour of the panel zone. (b) deformation of joint No. 9 at $\theta_{total} = 45\,mrad$. → stiffening of the composite column allowed for full activation of the connection → column stronger than connection.

For the above reason, it was decided to strengthen the rest of composite columns with additional cover plates welded on the outer side of the column flanges, see Figure 8b. This strengthening was judged as necessary in order to activate the connection and to render it the weakest component of the joint, but also in order to conform with basic principles of seismic design. In such way, the tested column configurations for the composite specimens were raised to 3: (i) all-steel HEA300 stiffened with supplementary web plates and stiffeners, see Figure 6b, (ii) steel-concrete composite columns, see Figure 6a & 8a, (iii) composite columns of the latter (2nd) configuration stiffened with additional cover plates on both sides, see Figure 8b.

The M-θ curve of specimen No. 6 (composite column) compared to a similar specimen with stiffened composite column, No. 9 is given in Figure 7 (Mc → measured moment of connection at column centreline). In fact, experiment No. 6 reached significantly lower values of moment $M^{+}_{exp.no.6} \approx 0{,}6 \cdot M^{+}_{exp.no.9}$, while testing was continued up to $\theta_{total} = 100\,mrad$ without mechanical failure of the connection or elsewhere, but with severe plastic deformations in the column panel zone, see Figure 8a and 7. On the contrary specimen No. 9 failed after having reached the moment capacity of the connection for $\theta_{total} = 50\,mrad$, see

Chapter 3.4.2 for failure mode and Chapter 3.3 for the contribution of the components to the total rotation. It should be noted that the requirement regarding minimum plastic rotation capacity of $\theta_{plastic} = 25\,mrad$ for partial strength joints implemented in medium seismicity areas according to [14] was satisfied by specimen No. 9. The hysteretic behaviour of the rest of composite specimens with stiffened composite column was generally similar to the one presented for experiment No. 9. Nevertheless, a distinct influence of the parameters has been observed through a systematic comparison between the experiments No. 7-11, see Table 1 and 2. A further study of the latter parameters with the help of FEM models will be part of [19].

Additionally, the behaviour of composite joints with 3 and 4 bolt rows was investigated with the help of experiments No. 5 and 12. Though for the 2 specimens the values of t_{ep} and e_4 are not identical, based on the rest experimental results, the number of bolt rows can be safely considered as the parameter with governing influence. The M-θ_{total} curves of experiments No. 5 and 12 are given in Figure 9.

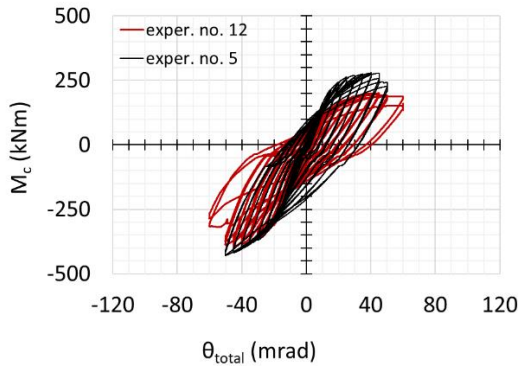

Figure 9 Comparison of M-θ_{total} curves for experiments No. 5 (3 bolt rows) & No. 12 (4 bolt rows). Lower sagging moments for experiment No. 12 but overall good hysteretic behaviour.

3.3 Contribution of the components beam & panel zone to the total rotation

Referring to the component contribution for the composite joints using the 1st column configuration (steel HEA300) there has been a sufficient activation of both the column web panel zone and the connection. Both specimens No. 12 (3 bolt rows) and No. 5 (4 bolt rows) showed an overall good hysteretic behaviour. The M-θ_b and M-γ curves for specimen No. 12 is given in Figure 10.

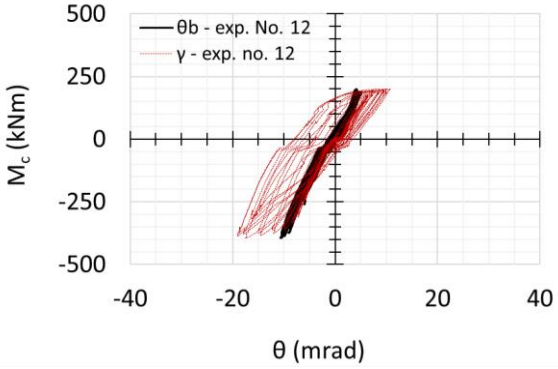

Figure 10 Contribution of the beam rotation and panel zone deformation, expressed through γ, to the total rotation of the joint.

The increased asymmetry of the composite connection through the use of 3 instead of 4 bolt rows in experiment No. 12 led to lower moment capacities for the connection under sagging moments but nevertheless, it showed a good dissipative behaviour with a good potential for use in low to medium seismicity areas. Especially, considering the under circumstances unexploited higher moment capacity for sagging moments of connections with 4 bolt rows, see also [18].

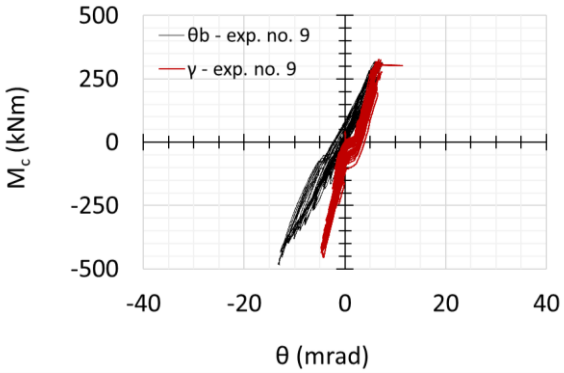

Figure 11 Contribution of the beam rotation and panel zone deformation, expressed through γ, to the total rotation of the joint. Stiffening of the column provided a strong column web panel which remained elastic throughout the test and allowed for full activation of the connection and subsequent investigation of its strength, stiffness and dissipative behaviour.

The contribution of panel zone and beam to the total rotation of the joint for a composite specimen, No. 9, is given in Figure 11. Additionally to the aforementioned contributions, also the concrete area around the shear studs and the studs themselves contribute to the hysteretic behaviour of the joint. That contribution was not measured herein and represents an additional source of energy dissipation. The concrete area around the first up to the third shear stud also was where the first cracks in the concrete slab formed, starting already from the first load step of $\theta_{total} = 3{,}75\,mrad$.

3.4 Failure mode

3.4.1 *All-steel joints*

Specimens No. 1 and No. 3 failed at $\theta_{total} = 70\,mrad$ and $\theta_{total} = 110\,mrad$ respectively. First a crack in the area of beam flange to endplate weld formed at $\theta_{total} = (60 - 70)\,mrad$, on the side of the endplate, without significant reduction of the moment strength. For very high rotation angles $\theta_{total} > 70\,mrad$ also bolt failures were observed. In the case of experiment No. 2, after the formation of a crack in the endplate, similar to experiment No. 1 and No. 3, a full plastic hinge formed in the beam. The test of experiment No. 2 was stopped at $\theta_{total} = 135\,mrad$, where the decrease at the moment was $M \approx 0{,}75 M_{ult.,connection}$.

3.4.2 *Composite joints*

Aside from the specimens No. 4 and 6 (unstiffened composite column), all other composite specimens failed with the formation of a crack in the area of beam flange to endplate welds on the side of beam flanges. The crack was initiated at around $\theta_{total} = 40\,mrad$, see Figure 12a, and developed until failure of the composite beam's steel section at maximum $\theta_{total} = 60\,mrad$, see Figure 12b. Failure crite-

rion was the formation of a crack longer than 2cm. Specimens tested at higher than the latter load steps showed a rapid development of the crack throughout the entire height of the steel beam section, see Figure 13a and 13b, while the concrete slab preserved its strength.

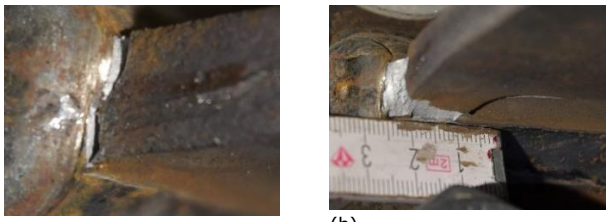

(a) (b)

Figure 12 (a) Crack initiation at a rotation of $\theta_{total} = 40\ mrad$ – weld at lower beam flange to endplate (b) crack propagation at a rotation of $\theta_{total} = 45\ mrad$.

(a) (b)

Figure 13 Crack grows throughout the entire height of the steel section of the composite beam for $\theta_{total} > 60\ mrad$.

Figure 14 Concrete crushing in the area of connection after the end of experiment No.10. Placement of first shear stud close to face of column → more intensive concrete cracking and crushing (at concrete cover).

The main cracks of the concrete slab were developed in the area around the shear studs, especially at the first up to third stud, and in the proximity of the connection where also concrete crushing of the concrete cover was observed, see Figure 14. The cracks of the concrete slab were generally of medium intensity, without significantly affecting its structural integrity.

4 Conclusions and critical discussion

The tested all-steel joints showed a highly ductile and good dissipative behaviour. The thickness of endplate t_{ep} and the vertical distance of the T-stub bolt rows e_4 were proven again, see [3] and [6], to have a significant influence on the joints´ behaviour. The variation of their values influences both the mechanical characteristics of the joints and their failure mode. Their good dissipative behaviour allows their use as dissipative joints in moment resisting frames of seismic resistant structures. Additionally, their highly ductile behaviour opens the possibility for application in structures designed for robustness, where alternative load paths are enabled after extreme events, e.g. loss of a column or even for multi-hazard scenarios as those described in [20]. The delayed activation of their hysteretic behaviour can possibly be dealt with larger beam profile sizes.

The tested composite joints on the other hand profited from the increased flexural stiffness of the composite beam. Their hysteretic behaviour started from $\theta_{total} = 10\ mrad$ and continued up to at least $\theta_{total} = 45\ mrad$. In such way, the energy dissipation capacity of the tested joints could be realistically and safely exploited in moment resisting frames of a real steel-concrete composite structure located in a low-to-medium seismicity area. The optimisation of the composite joints presented here, by means of a haunch on the lower side of the joint in combination with a weaker concrete slab that allows for a better activation of the endplate can provide higher levels of energy dissipation and ductility that are required in high-seismicity areas.

Referring to the columns of the composite specimens, the stiffened composite configuration performed well, had a strong web panel and allowed for full activation of the connections. The all-steel stiffened one presented also a good performance, with a balanced column web panel zone that contributed to the energy dissipation. The composite column configuration effectively prevented significant cracking in the concrete core for up to at least $\theta_{total} = 45\ mrad$ but did not allow for full activation of connection. It needs improvements, further investigations should use stronger steel profile series, i.e. HEB or HEM series for the column.

A report for the 12 tests will become available in [1]. Additionally, FEM models of both the all-steel and composite joints together with different parameter studies, a methodology for the design of partial-strength joints as dissipative ones and a ductility criterion, based on a deformation capacity approach, for partial-strength joints with a failure mode 2 are in preparation in [19].

5 Acknowledgements

The experiments were performed at the Materials Testing Institute of University of Stuttgart as part of [1] and financed through the Research Association for Steel Application (FOSTA), the German Federation of Industrial Research Associations (AiF) and the German Federal Ministry of Economic Affairs and Climate Action. The joint project is carried out at the Institute of Structural Design of the University of Stuttgart and at the Centre for Wind and Earthquake Engineering of RWTH-Aachen University.

References

[1] B. Hoffmeister; G. Balaskas; R. Don; C. Vulcu; U. Kuhlmann; G. Skarmoutsos, "(IGF no. 21383 N/1 / FOSTA-P-1481) Entwicklung von standartisierten Stützen-Riegel-Anschlüssen für Stahl- und Verbundkonstruktionen in deutschen Erdbebengebieten (development of standardised steel and steel-concrete beam-to-column joints for seismic areas in Germany)", in prep..

[2] U. Kuhlmann; L. Rölle; J. P. Jaspart; J. F. Demonceau; O. Vassart; K. Weynand; C. Ziller; E. Busse; M. Lendering; R. Zandonini; N. Baldassino, "Robust structures by joint ductility, Final report of the project RFSR-CT-2004-00046," European

Commission, Brussels, 2009.

[3] U. Kuhlman; L. Rölle, "Duktilitätskriterien für typisierte Stirnplattenverbindungen (ductility criteria for standardised endplate connections)", Deutscher Ausschuss für Stahlbau DASt, 2008.

[4] U. Kuhlmann; N. Hoffmann; J. P. Jaspart; J. F. Demonceau; R. Zandonini; N. Baldassino; B. Hoffmeister; C. Colomer; C. Korndörfer; F. Hanus; M. Charlier; M. Hjiaj; S. Guezouli, "Robust impact design of steel and composite building structures (ROBUSTIMPACT), Grant Agreement RFSR-CT-2012-00029," European Commission, Brussels, 2017.

[5] M. Schäfer, "*Zum Rotationsnachweis teiltragfähiger Verbundknoten in verschieblichen Verbundrahmen (About rotation capacity verification of partial-strength steel-concrete composite joints of sway frames)",* Stuttgart: Dissertation - Institute of Structural Design, University of Stuttgart, 2005.

[6] L. Rölle, "*Das Trag- und Verformungsverhalten geschraubter Stahl- und Verbundknoten bei vollplastischer Bemessung und in außergewöhnlichen Bemessungssituationen (The load carrying and deformation behaviour of bolted steel and steel-concrete composite joints for full plastic design and for extreme load cases)",* Stuttgart: Dissertation - Institute of Structural Design, University of Stuttgart, 2013.

[7] N. Keller, "*Robustheit von Stahl- und Verbundrahmendurch gezielte Anschlussausbildung (Design of joints for robust behaviour of steel and steel-concrete frames)",* Stuttgart: Dissertation - Institute of Structural Design, University of Stuttgart, 2019.

[8] R. Landolfo; F. Mazzolani; D. Dubina; L. S. da Silva; M. D´Aniello, Design of Steel Structures for Buildings in Seismic Areas, ECCS Eurocode Design Manuals, ECCS - European Convention for Constructional Steelwork, 2017.

[9] R. Landolfo; M. D' Aniello; S. Costanzo; R. Tartaglia; A. Stratan; D. Dubina; C. Vulcu; C. Maris; C. Zub; L. Da Silva; C. Rebelo; H. Augusto; A. Shahbazian; F. Gentili; J.-P. Jaspart; J.-F. Demonceau; L. Van Hoang; A. Elghazouli; A. Tsitos; O. Vassart; E. M. Nunez; V. Dehan; C. Hamreza, "European pre-QUALified steel JOINTS (EQUALJOINTS): Final Report of the project RFSR-CT-2013-00021," European Commission, Brussels, 2017.

[10] U. Kuhlmann; L. Rölle; N. Hoffmann, "Verbundanschlüsse nach Eurocode (steel-concrete composite joints according to the Eurocode)," in *Stahlbaukalender 2018*, U. Kuhlmann, Editor, 2018,

[11] J. P. Jaspart; K. Weynand, Design of Joints in Steel and Composite Structures, ECCS Eurocode Design Manuals, ECCS - European Convention for Constructional Steelwork, 2016.

[12] CEN EN 1993-1-8, Eurocode 3: Design of steel structures-Part 1-8: Design of joints, Brussels: European Committee for Standardization, 2005.

[13] CEN EN 1994-1-1, Eurocode 4: Design of composite steel and concrete structures, Brussels: European Committee for Standardization, 2009.

[14] CEN EN 1998-1, Eurocode 8: Design of structures for earthquake resistance, Brussels: European Committee for Standardization, 2010.

[15] AISC (2016a), "Seismic provisions for structural steel buildings." ANSI/AISC 341-16, Chigago, Illinois: American Institute for Steel Construction, 2016a.

[16] AISC (2016c), Prequalified Connections for special and intermediate steel moment frames for seismic applications, ANSI/AISC 358-16, Chicago, Illinois: American Institute for Steel Construction, 2016.

[17] FEMA 461 (2007), Interim Testing Protocols for Determining the Seismic Performance Characteristics of Structural and Nonstructural Components, Washington D.C.: Federal Emergency Management Agency, 2007.

[18] G. Skarmoutsos; U. Kuhlmann, "Dissipative steel and steel-concrete composite beam-to-column joints," in *Proceedings of eighth international symposium on life-cycle civil engineering-IALCCE2023*, Milan, Italy, Taylor & Francis, (in preparation - July 2023).

[19] prCEN/TS 1998-1-101, Eurocode 8 - Design of structures for earthquake resistance - part 1-101 Characterisation and qualification of structural components for seismic applications by means of cyclic tests, Brussels: European Committee for Standardization, 2023.

[20] G. Skarmoutsos, "*Dissipative all-steel and steel-concrete composite joints",* Dissertation: Institute of Structural Design, University of Stuttgart, in prep..

[21] J. F. Demonceau; T. Golea; J. P. Jaspart; A. Elghazouli; Z. Khalil; A. Santiago; A. F. Santos; L. Simoes da Silva; U. Kuhlmann; G. Skarmoutsos; N. Baldassino; R. Zandonini; M. Bernardi; M. Zordan; F. Dinu; I. Marginean; D. Jakab; D. Dubina; F. Wertz; K. Weynand; R. Obiala; M. Candeias; M. Charlier; O. Anwaar, "Design recommendations against progressive collapse in steel and steel-concrete buildings (FAILNOMORE)", ECCS - European Convention for Constructional Steelwork, Brussels, Belgium, 2021.